

# Multifunctional PEG encapsulated $\text{Fe}_3\text{O}_4@\text{silver}$ hybrid nanoparticles: antibacterial activity, cell imaging and combined photothermo/chemo-therapy

Hui Wang<sup>a</sup>, Jing Shen<sup>a</sup>, Guixin Cao<sup>b</sup>, Zheng Gai<sup>b</sup>, Kunlun Hong<sup>b</sup>, Priya R. Debata<sup>a</sup>, Probal Banerjee<sup>a</sup>, Shuiqin Zhou<sup>a\*</sup>

<sup>a</sup>Department of Chemistry, The College of Staten Island, and The Graduate Center, The City University of New York, Staten Island, NY 10314; <sup>b</sup>Center for Nanophase Materials Sciences and Chemical Science Division, Oak Ridge National Laboratory, Oak Ridge, TN 37831, USA

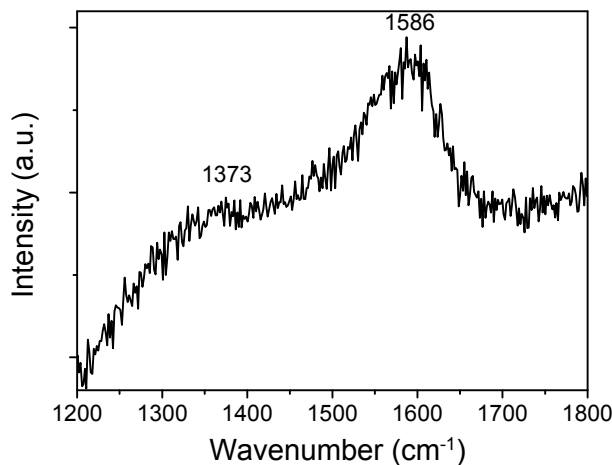


Fig. S1. Raman spectrum of the as-obtained  $\text{Fe}_3\text{O}_4@\text{PEG}$  NPs.

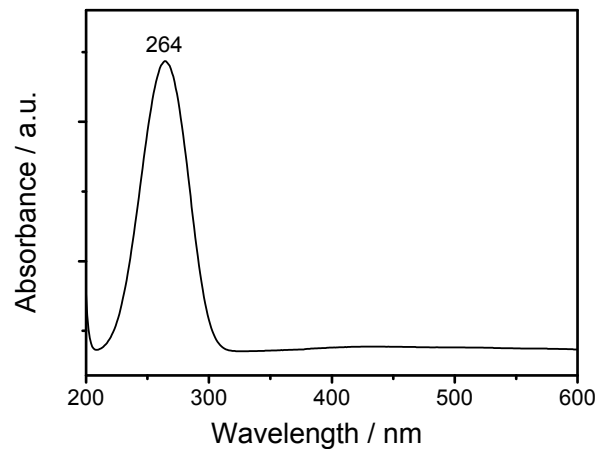


Fig. S2. Typical UV-visible absorption spectrum of the as-obtained  $\text{Fe}_3\text{O}_4@\text{PEG}$  NPs.

\* Corresponding authors. E-mail address: shuiqin.zhou@csi.cuny.edu; Tel.: +1 718 982 3897; Fax: +1 718 982 3910.

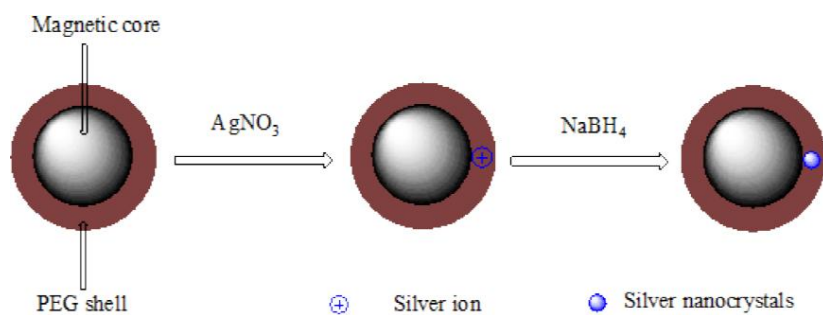


Fig. S3. Schematic illustration of the synthesis of Fe<sub>3</sub>O<sub>4</sub>@Ag-PEG hybrid NPs.

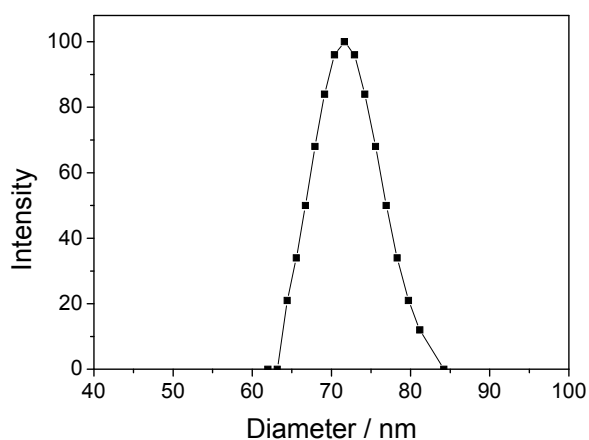


Fig. S4. Hydrodynamic diameter distribution of the Fe<sub>3</sub>O<sub>4</sub>@Ag-PEG hybrid NPs synthesized at 30 °C and [Ag<sup>+</sup>] = 0.19 mM for 1h.

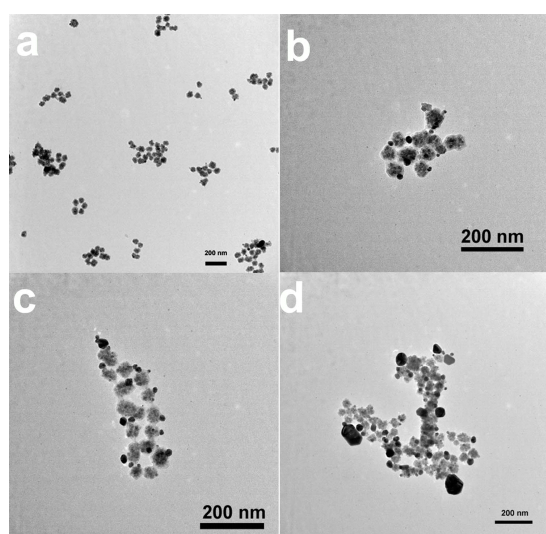


Fig. S5. TEM images of the Fe<sub>3</sub>O<sub>4</sub>@Ag-PEG hybrid NPs synthesized at 30 °C and initial [Ag<sup>+</sup>] = 0.19 mM, but for different reaction time: (a) 1 h, (b) 3 h, (c) 6 h, and (d) 12 h.

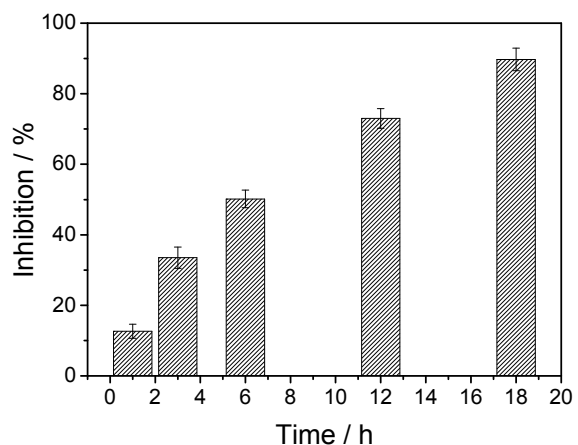


Fig. S6 The bacterial inhibition efficiency of the dumbbell-like structured  $\text{Fe}_3\text{O}_4@\text{Ag}$ -PEG hybrid NPs (the average size of Ag NPs = 22 nm, concentration = 160  $\mu\text{g}/\text{mL}$ ) at different interaction time with bacteria.

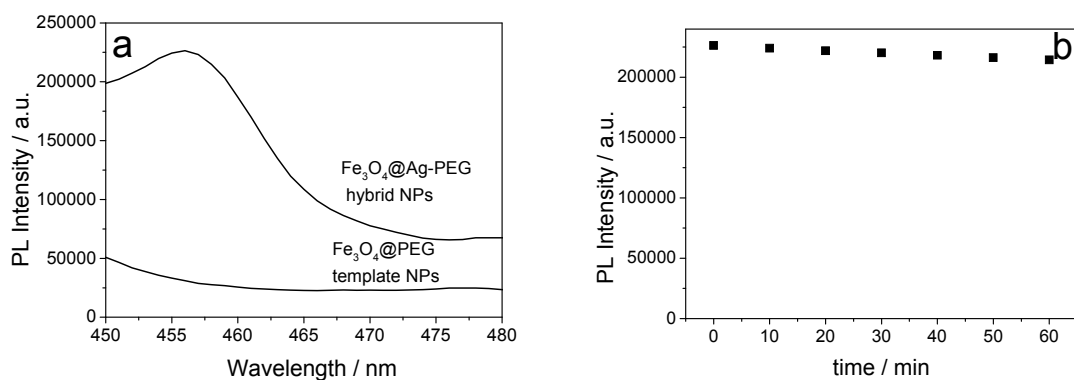


Fig. S7. (a) The PL spectra of the  $\text{Fe}_3\text{O}_4@\text{PEG}$  template NPs and  $\text{Fe}_3\text{O}_4@\text{Ag}$ -PEG hybrid NPs synthesized at  $[\text{Ag}^+] = 0.19 \text{ mM}$  and  $30^\circ\text{C}$  for 1 h. (b) The fluorescence intensity of the  $\text{Fe}_3\text{O}_4@\text{Ag}$ -PEG hybrid NPs used in (a) under different excitation time. Excitation wavelength = 390 nm.

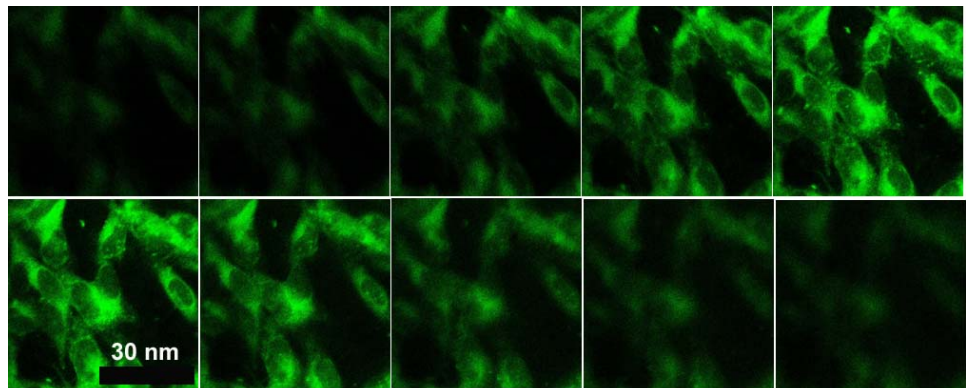


Fig. S8. Z-Scanning confocal fluorescence images of the B16F10 cells incubated with the  $\text{Fe}_3\text{O}_4@\text{Ag}$ -PEG hybrid NPs containing multiple Ag nanocrystals in the shell. Excitation wavelength = 405 nm.

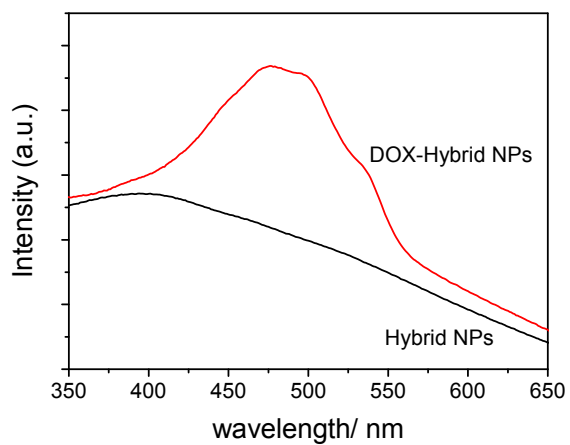


Fig. S9. Typical UV-visible absorption spectra of the as-obtained  $\text{Fe}_3\text{O}_4@\text{Ag}$ -PEG hybrid NPs and DOX-loaded  $\text{Fe}_3\text{O}_4@\text{Ag}$ -PEG hybrid NPs.

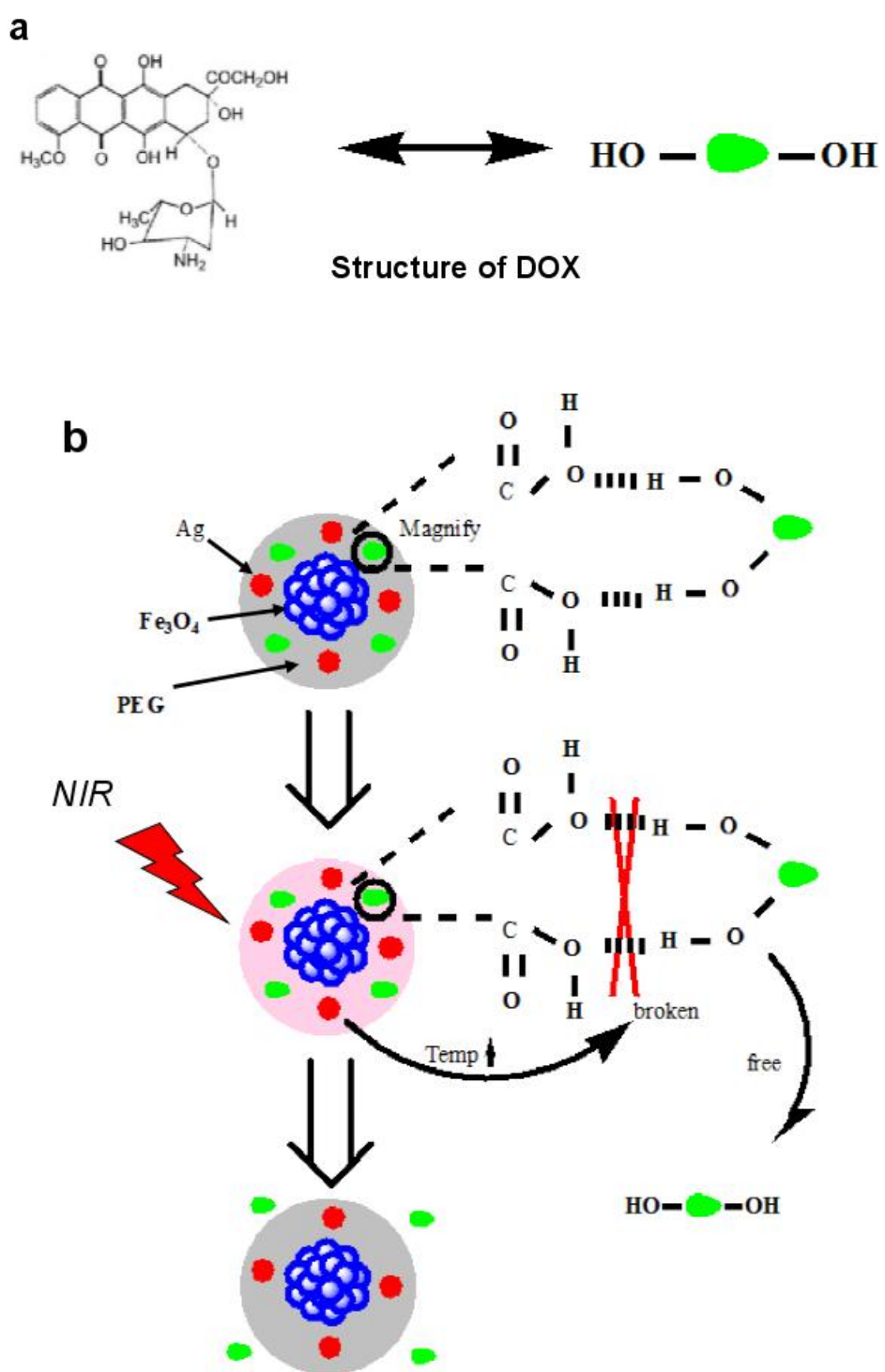


Fig. S10 (a) Structure of DOX; (b) Schematic illustration of the NIR photo-controlled drug release from the DOX-loaded  $\text{Fe}_3\text{O}_4@\text{Ag}$ -PEG hybrid NPs.

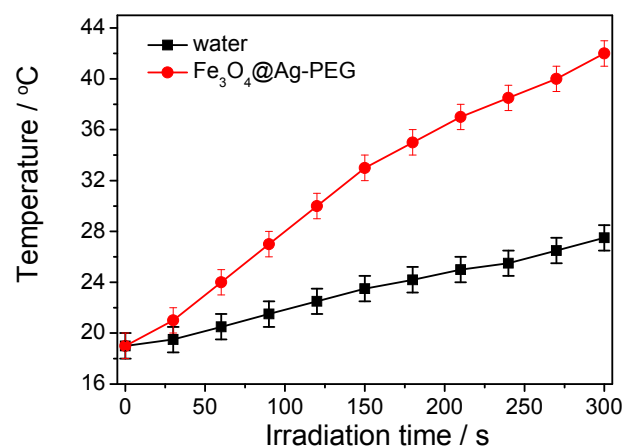


Fig. S11. The heating curves of water and Fe<sub>3</sub>O<sub>4</sub>@Ag-PEG (0.2 mg/mL) hybrid NPs under NIR irradiation.

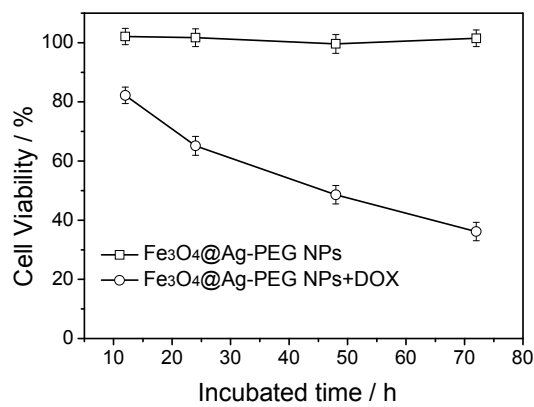


Fig. S12 In vitro cytotoxicity of B16F10 cells incubated with DOX-free Fe<sub>3</sub>O<sub>4</sub>@Ag-PEG NPs and DOX-loaded Fe<sub>3</sub>O<sub>4</sub>@Ag-PEG NPs under different incubation time.

**Table S1.** The loading content of Ag nanocrystals in and/or on the Fe<sub>3</sub>O<sub>4</sub>@Ag-PEG hybrid NPs

Initial concentration [Ag <sup>+</sup> ]/ mM	Remanent concentration [Ag <sup>+</sup> ]/ mM	Loading content
0.19	0.0038	98%
0.38	0.0256	93%
0.58	0.1276	78%